

## *Supplement for:*

# **Variation in chemical composition and volatility of oxygenated organic aerosol in different rural, urban, and remote environments**

5 Wei Huang<sup>1</sup>, Cheng Wu<sup>2,3</sup>, Linyu Gao<sup>4</sup>, Yvette Gramlich<sup>2,5</sup>, Sophie L. Haslett<sup>2,5</sup>, Joel Thornton<sup>6</sup>,  
Felipe D. Lopez-Hilfiker<sup>7</sup>, Ben H. Lee<sup>6</sup>, Junwei Song<sup>4</sup>, Harald Saathoff<sup>4</sup>, Xiaoli Shen<sup>4,8</sup>,  
Ramakrishna Ramisetty<sup>4,9</sup>, Sachchida N. Tripathi<sup>10</sup>, Dilip Ganguly<sup>11</sup>, Feng Jiang<sup>4</sup>, Magdalena  
Vallon<sup>4</sup>, Siegfried Schobesberger<sup>12</sup>, Taina Yli-Juuti<sup>12</sup>, Claudia Mohr<sup>2,5,13,\*</sup>

10 <sup>1</sup>Institute for Atmospheric and Earth System Research / Physics, Faculty of Science, University of Helsinki, 00014,  
Helsinki, Finland

<sup>2</sup>Department of Environmental Science, Stockholm University, 11418, Stockholm, Sweden

<sup>3</sup>Now at: Department of Chemistry and Molecular Biology, University of Gothenburg, 41296, Gothenburg, Sweden

<sup>4</sup>Institute of Meteorology and Climate Research, Karlsruhe Institute of Technology, 76344, Eggenstein-Leopoldshafen,  
Germany

15 <sup>5</sup>Bolin Centre for Climate Research, Stockholm University, 11418, Stockholm, Sweden

<sup>6</sup>Department of Atmospheric Sciences, University of Washington Seattle, Washington 98195, United States

<sup>7</sup>Tofwerk AG, 3600 Thun, Switzerland

<sup>8</sup>Now at: Department of Earth, Atmospheric, and Planetary Sciences, Purdue University, West Lafayette, Indiana  
47907, United States

20 <sup>9</sup>Now at: TSI Instruments India Private Limited, 560102, Bangalore, India

<sup>10</sup>Department of Civil Engineering, Indian Institute of Technology Kanpur, 208016, Kanpur, India

<sup>11</sup>Centre for Atmospheric Sciences, Indian Institute of Technology Delhi, 110016, New Delhi, India

<sup>12</sup>Department of Technical Physics, University of Eastern Finland, 70211, Kuopio, Finland

25 <sup>13</sup>Now at: Department of Environmental System Science, ETH Zurich and Laboratory of Atmospheric Chemistry, Paul  
Scherrer Institute, 5232 Villigen, Switzerland

\*Correspondence to: Claudia Mohr ([claudia.mohr@psi.ch](mailto:claudia.mohr@psi.ch))

**Table S1.** Campaign-average (average  $\pm$  1 standard deviation) parameters for meteorology, trace gases, equivalent black carbon (eBC), total organics and total PM<sub>2.5</sub>, double bond equivalent (DBE) values, and number of carbon atoms (nC) and oxygen atoms (nO) at different locations and different seasons.

Name	T (°C)	RH (%)	O <sub>3</sub> (ppbv)	NO <sub>2</sub> (ppbv)	SO <sub>2</sub> (ppbv)	eBC (µg m <sup>-3</sup> )	Org <sup>a</sup> (µg m <sup>-3</sup> )	PM <sub>2.5</sub> <sup>a</sup> (µg m <sup>-3</sup> )	DBE	nC	nO
MCC-t	0.3±2.1	53.0±22.4	/	/	/	0.2±0.4	0.3±0.5	1.0±1.8	3.1±0.2	8.4±0.8	6.2±0.3
MCC-d	-0.4±1.9	52.2±18.8	/	/	/	0.3±0.4	0.5±0.5	1.6±1.4	3.2±0.1	7.7±0.7	5.8±0.3
REL	19.9±3.9	76.1±15.2	22.7±12.4	11.3±5.2	1.4±1.0	0.7±0.4	3.7±2.1	6.6±4.2	3.1±0.1	9.2±0.8	6.6±0.5
RAB	24.2±3.2	83.1±15.2	25.0±12.5	0.6±0.6	0.2±0.4	/	4.1±2.5	6.0±3.2	2.9±0.1	8.0±0.4	5.7±0.2
RHT	8.1±6.1	66.0±23.7	36.1±10.1	0.4±0.6	0.2±0.2	0.1±0.2	1.6±2.0	2.3±2.3	3.1±0.1	9.1±0.6	5.7±0.3
UST-s	24.6±4.0	55.1±12.8	29.6±7.5	9.7±4.1	3.9±2.8	1.0±0.3	5.1±3.2	7.1±3.3	3.4±0.1	8.8±0.4	6.4±0.2
UST-w	2.0±3.7	61.4±10.1	17.1±8.7	15.8±3.9	1.4±0.8	1.2±0.1	8.4±5.6	27.0±11.9	3.4±0.1	8.7±0.9	6.7±0.2
UKA-s	25.9±6.6	49.8±21.0	37.4±19.8	9.6±6.4	/	0.7±0.4	3.9±2.4	5.9±2.8	3.6±0.2	10.7±0.8	7.0±0.4
UKA-w	13.2±3.3	56.4±13.4	27.8±10.0	9.2±7.1	0.6±1.0	0.5±0.5	1.9±1.6	3.9±3.6	3.5±0.1	11.2±0.8	7.1±0.4
UDL	16.8±4.1	73.3±16.7	11.1±13.3	34.6±22.0	/	16.1±13.3	86.4±66.7	172.7±103.8	4.0±0.2	9.4±0.4	4.9±0.1

<sup>a</sup>Data were total non-refractory mass concentration from a high-resolution time-of-flight aerosol mass spectrometer (HR-ToF-AMS, Aerodyne Research Inc.) or an aerosol chemical speciation monitor (ACSM, Aerodyne Research Inc.).

**Table S2.** Deposition parameters and instrumental parameters at different locations and different seasons.

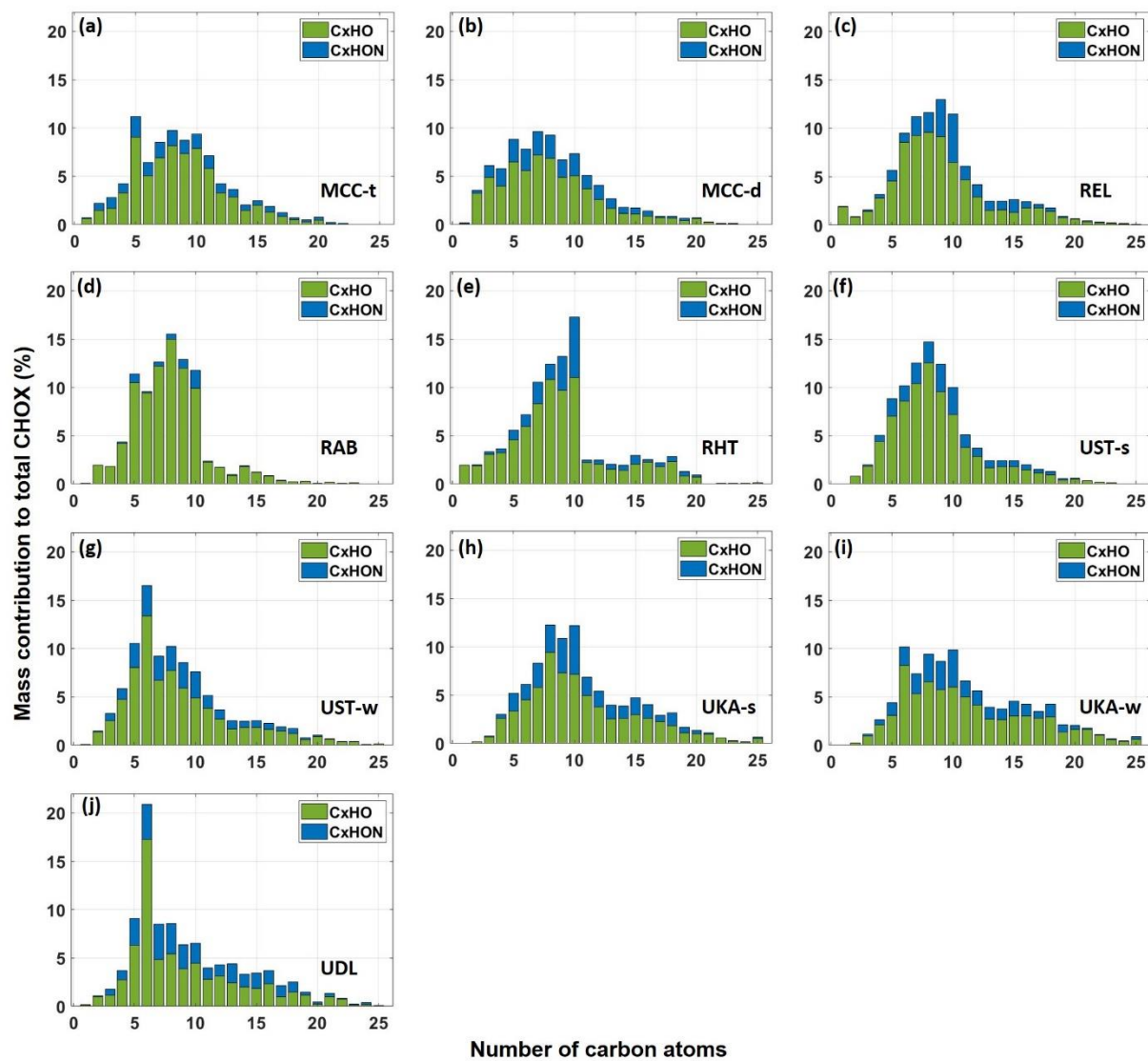
Name	Total inlet flow (L/min)/ Residence time (s)		Deposition time (min)	Mass loading ( $\mu\text{g}$ ) <sup>c</sup>	FIGAERO type/ Sample mode	IMR body T (°C)	IMR pressure (mbar)	Ion source	Ratio sample flow : ionizer flow	Ramp rate (°C/min)
MCC-t	7.0/1.4		120	0.3±0.3	Aerodyne/online	45	100	Corona discharge	2:1.3	13.3
MCC-d	7.0/1.4		120	0.4±0.4	Aerodyne/online	45	480	X-ray	2:1.3	13.3
REL	8.6/1.2		30	1.0±0.7	Aerodyne/online	45	100	Po-210	2:2	13.3
RAB	22/3.6		20	1.8±1.3	UW/online <sup>d</sup>	25	100	Po-210	2:2	10.0
RHT	11/4.2		30	0.5±0.8	UW/online <sup>d</sup>	25	100	Po-210	2:2	10.0
UST-s	8.7/0.8		112±43 <sup>b</sup>	3.5±1.4	Aerodyne/offline	45	100	Po-210	2:2	13.3
UST-w	10.0/0.7		86±70 <sup>b</sup>	4.0±1.0	Aerodyne/offline	45	100	Po-210	2:2	13.3
UKA-s	6.4/0.8		128±99 <sup>b</sup>	3.2±2.1	Aerodyne/offline	45	100	Po-210	2:2	13.3
UKA-w	6.4/0.8		245±124 <sup>b</sup>	3.0±1.5	Aerodyne/offline	45	100	Po-210	2:2	13.3
UDL	2.4 <sup>a</sup> /2.8		3±1	0.6±0.5	Aerodyne/online	25	250	X-ray	2:1.5	6.7

<sup>a</sup>Average inlet flow of 3.5 L/min for the 1<sup>st</sup> week and 2 L/min for the next 2.5 weeks.

<sup>b</sup>Deposition time was average ± 1 standard deviation from offline filters.

<sup>c</sup>Mass loadings were calculated based on concurrent HR-ToF-AMS or ACSM measurements.

<sup>d</sup>FIGAERO inlet from the University of Washington, U.S., designed by Lopez-Hilfiker et al. (2014).



30 **Figure S1.** Mass contributions of CHO and CHON compounds to total CHOX compounds as a function of the number of carbon atoms for MCC-t (a), MCC-d (b), REL (c), RAB (d), RHT (e), UST-s (f), UST-w (g), UKA-s (h), UKA-w (i), and UDL (j).

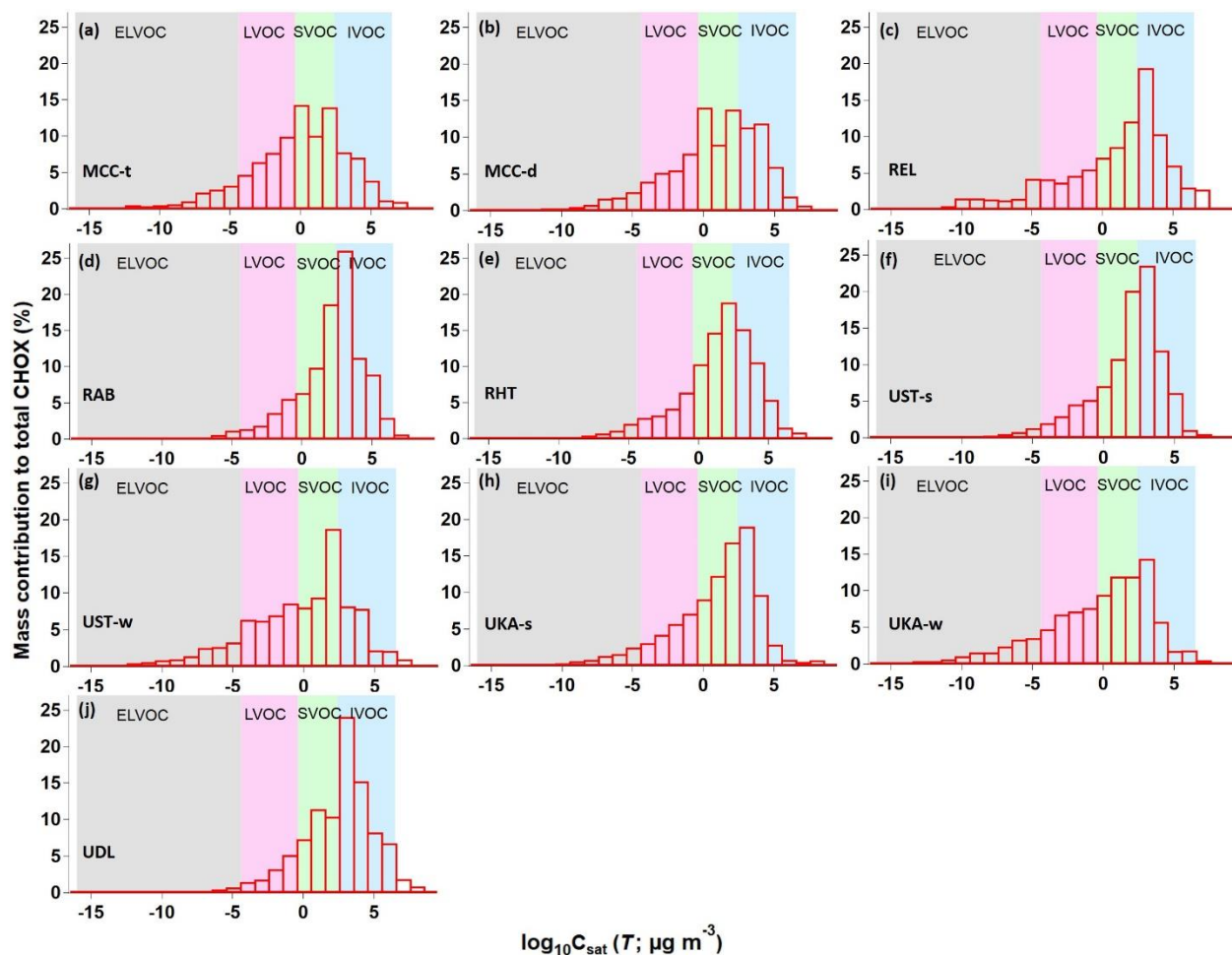


**Figure S2.** Volatility distribution for MCC-t (a), MCC-d (b), REL (c), RAB (d), RHT (e), UST-s (f), UST-w (g), UKA-s (h), UKA-w (i), and UDL (j) with the modified Li et al. (2016) parameterization method (Daumit et al., 2013; Isaacman-VanWertz and Aumont, 2021).

35

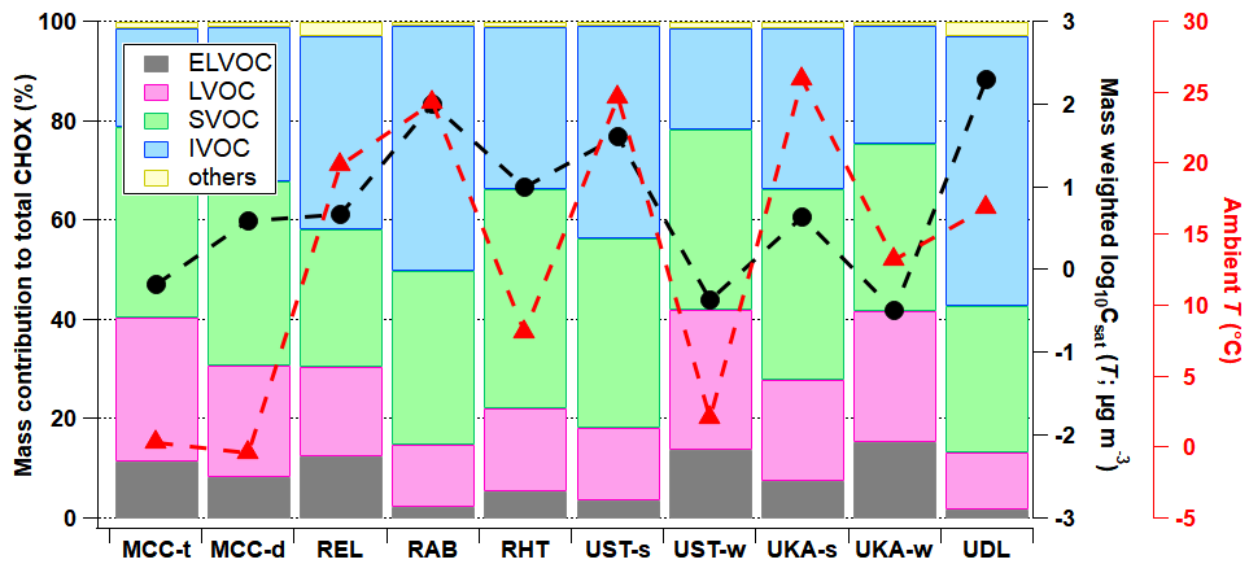


**Figure S3.** Comparison between ambient temperature ( $T$ ) and campaign-average contribution (%) of different volatility groups resulting from VBS calculations to total organics (colored in bars) and campaign-average mass weighted  $\log_{10}C_{\text{sat}}(T)$  values (in black markers) for different campaigns with the modified Li et al. (2016) parameterization method (Daumit et al., 2013; Isaacman-VanWertz and Aumont, 2021) (same as Figure 2). Compounds more volatile than IVOC with  $C_{\text{sat}}$  higher than  $10^{6.5} \mu\text{g m}^{-3}$  (labelled as “others”) contributed negligibly (0.8–2.9%).

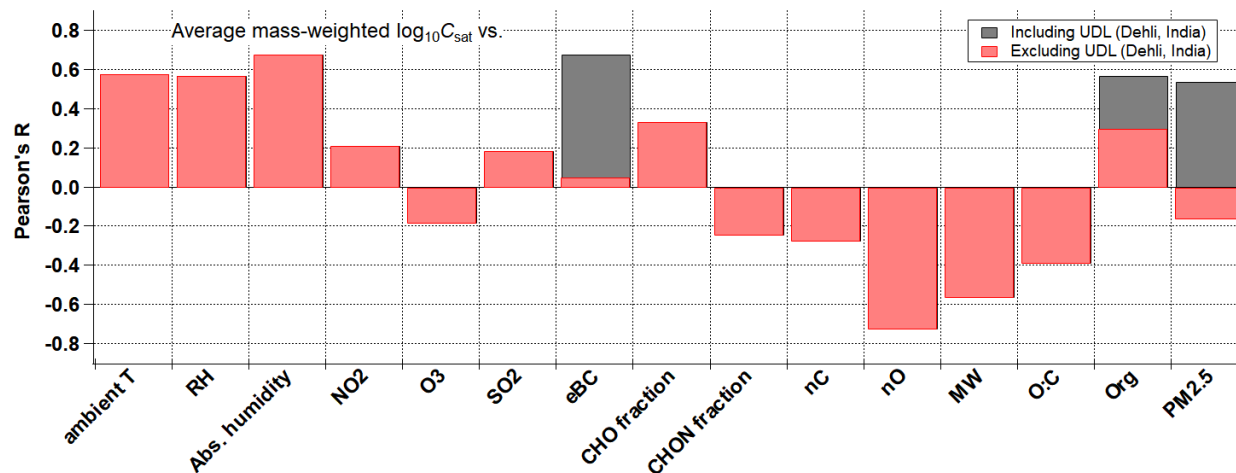


**Figure S4.** Correlations of campaign-average mass weighted  $\log_{10}C_{\text{sat}}$  values vs. other parameters. Pearson's R values including and excluding UDL (Dehli, India) data point for eBC, Org, and PM<sub>2.5</sub> are in gray bars and red bars, respectively, due to their extremely high levels at UDL (see Table S1).

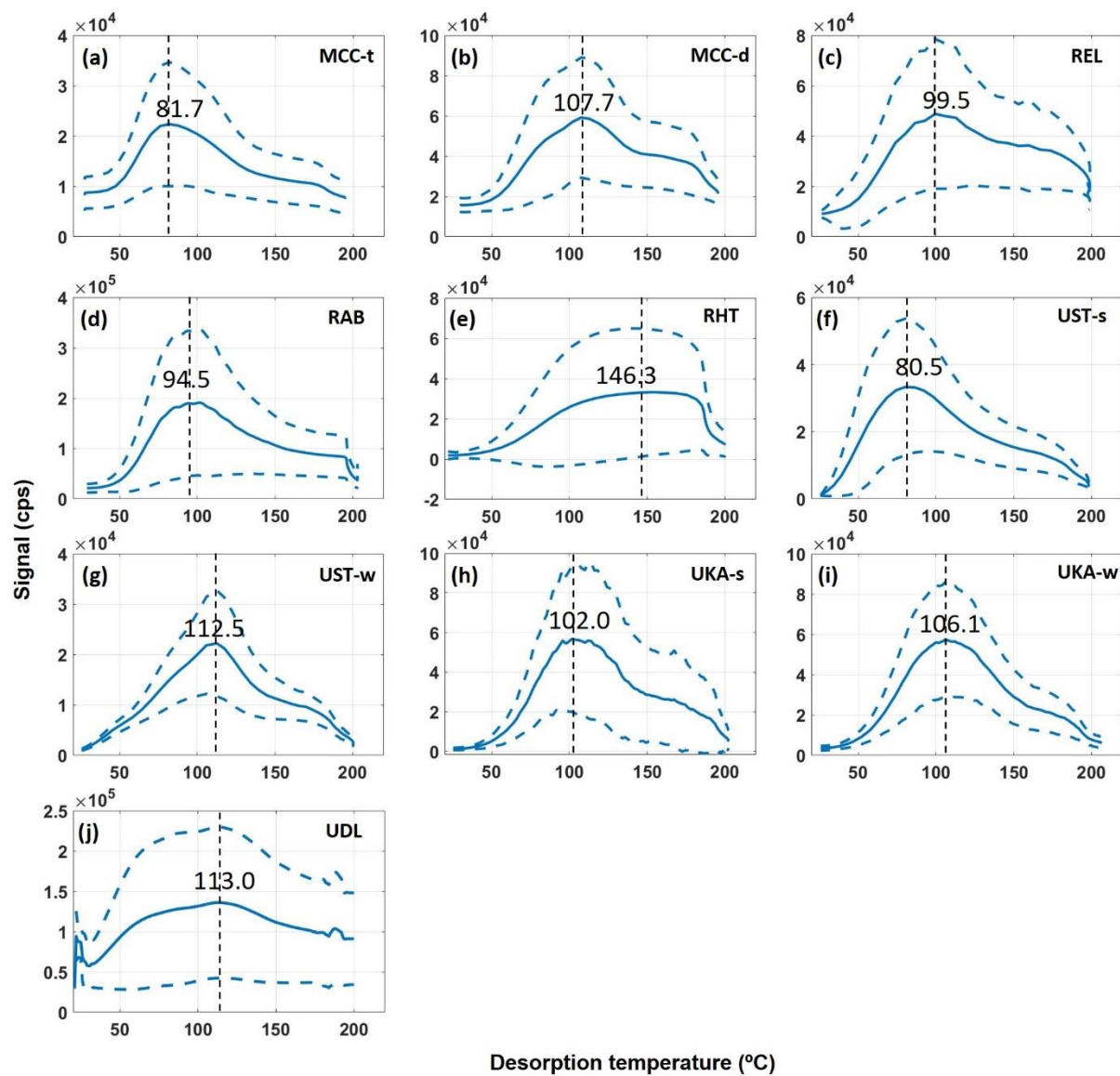


**Figure S5.** Campaign-average sum thermograms of CHOX compounds for MCC-t (a), MCC-d (b), REL (c), RAB (d), RHT (e), UST-s (f), UST-w (g), UKA-s (h), UKA-w (i), and UDL (j). Dashed blue lines represent  $\pm 1$  standard deviation and dashed black lines indicate the  $\text{sumT}_{\text{max}}$  values.

50



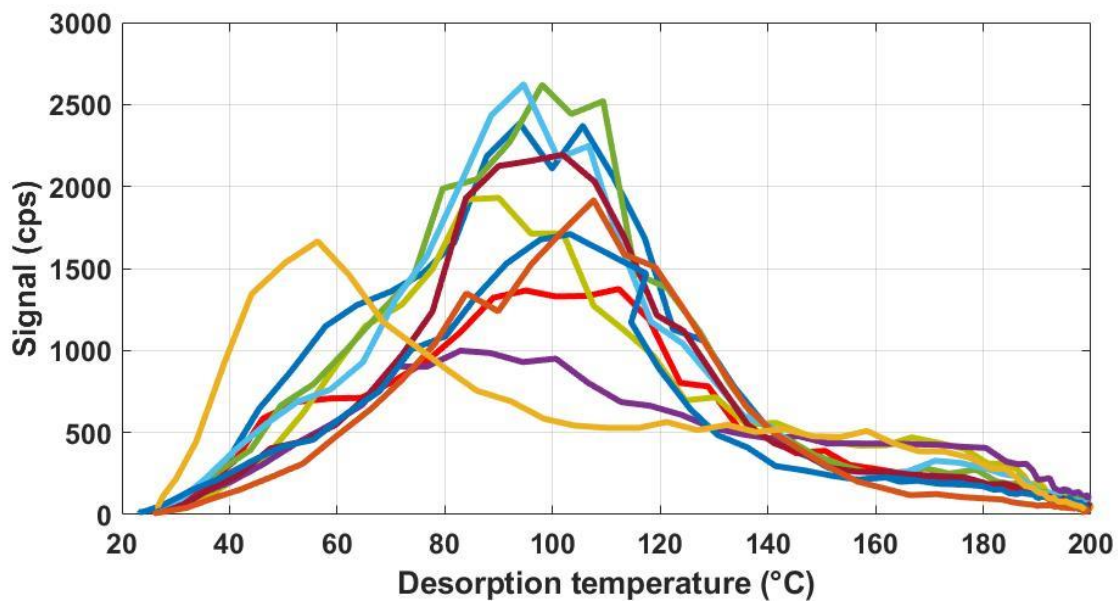


**Figure S6.** Thermograms of  $C_6H_{10}O_5$  compound during the whole campaign in winter Stuttgart (UST-w).

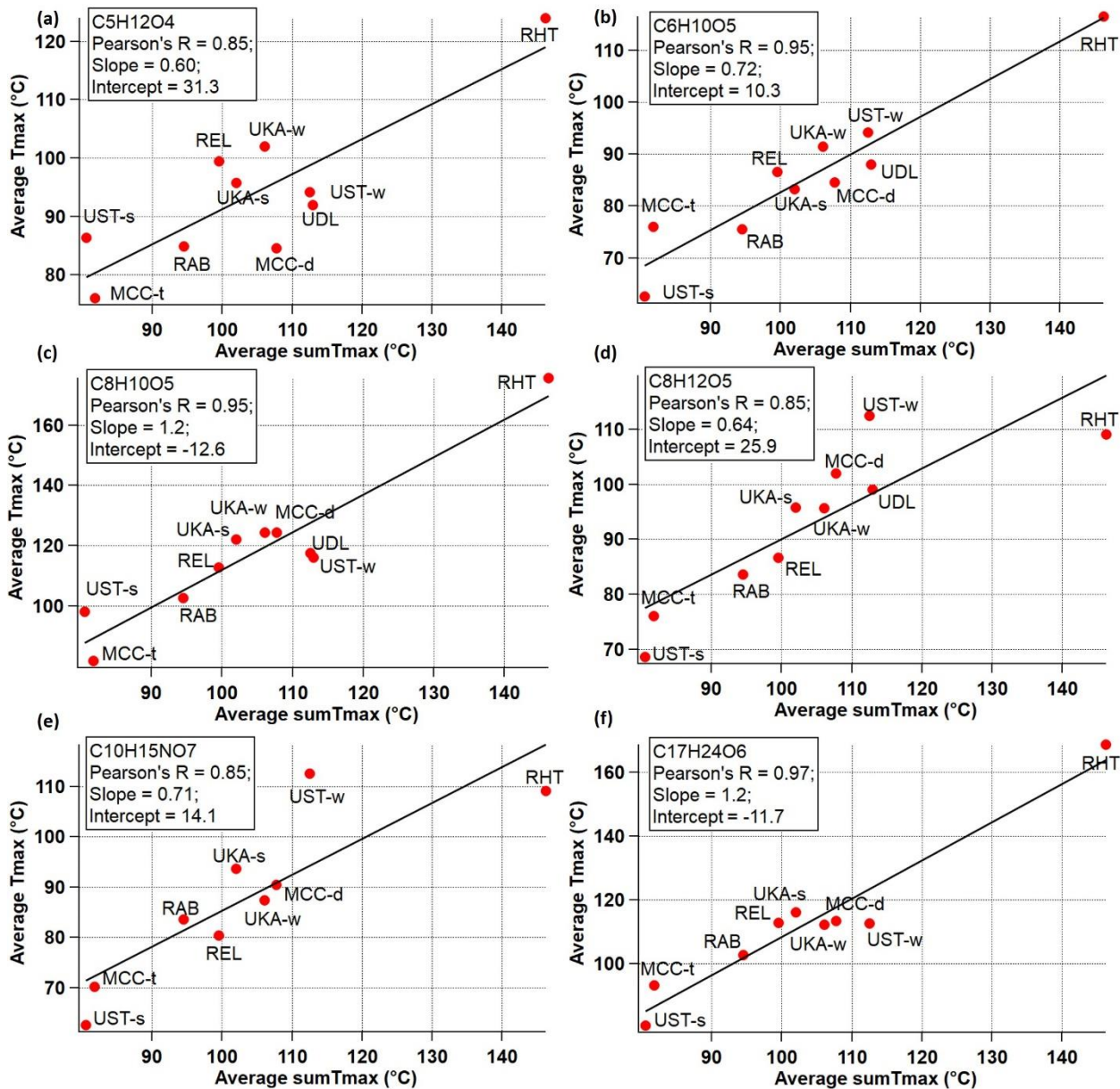


**Figure S7.** Campaign-average  $T_{\max}$  values for  $\text{C}_5\text{H}_{12}\text{O}_4$  (a),  $\text{C}_6\text{H}_{10}\text{O}_5$  (b),  $\text{C}_8\text{H}_{10}\text{O}_5$  (c),  $\text{C}_8\text{H}_{12}\text{O}_5$  (d),  $\text{C}_{10}\text{H}_{15}\text{NO}_7$  (e), and  $\text{C}_{17}\text{H}_{24}\text{O}_6$  (f) vs. the corresponding campaign-average  $\text{sum}T_{\max}$  values.

55

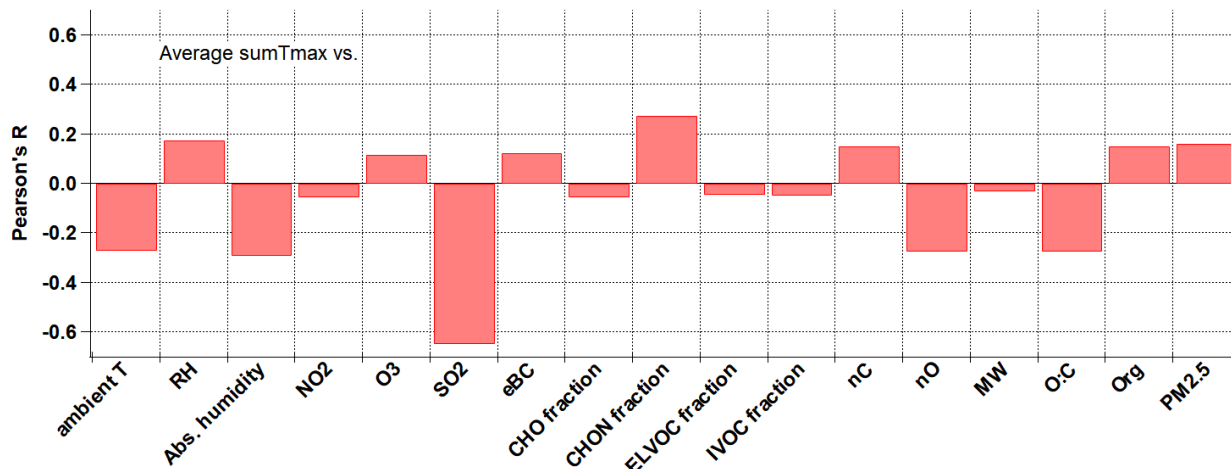
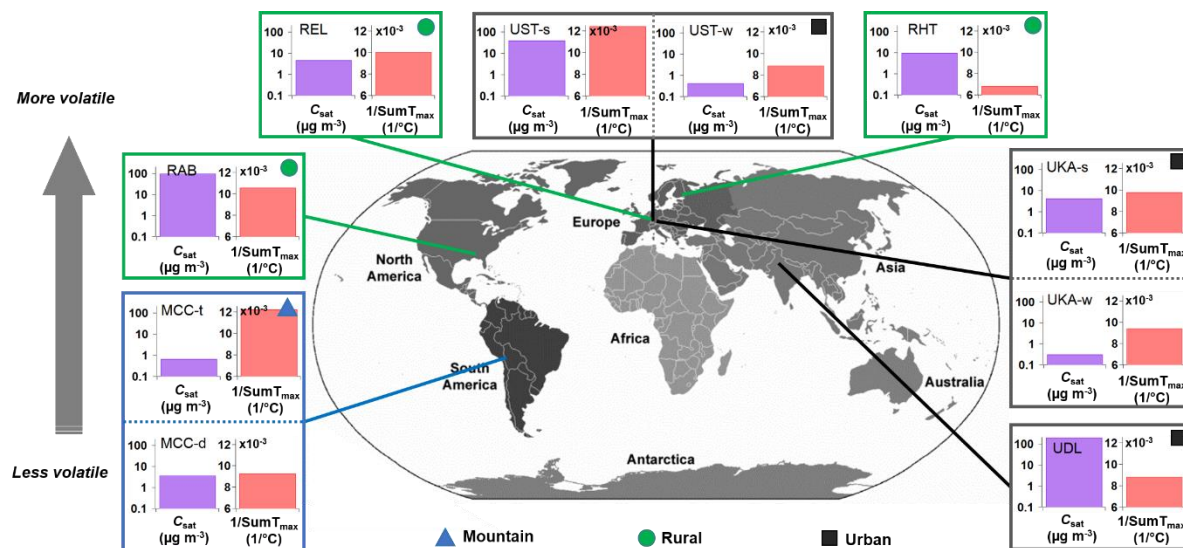


**Figure S8.** Correlations of campaign-average sumT<sub>max</sub> values vs. other parameters.



60 **Figure S9.** Overview of the comparison of the average  $C_{sat}(T)$  (i.e., molecular composition-derived volatility) with the  $\text{sumT}_{max}$  (i.e., thermal desorption-derived volatility) for different locations and seasons (Mountain sites in triangles, Rural sites in circles, and Urban sites in squares).

## References

- Daumit, K. E., Kessler, S. H., and Kroll, J. H.: Average chemical properties and potential formation pathways of highly oxidized organic aerosol, *Faraday Discuss*, 165, 181-202, <https://doi.org/10.1039/C3FD00045A>, 2013.
- 65 Isaacman-VanWertz, G., and Aumont, B.: Impact of organic molecular structure on the estimation of atmospherically relevant physicochemical parameters, *Atmos Chem Phys*, 21, 6541–6563, <https://doi.org/10.5194/acp-21-6541-2021>, 2021.
- Li, Y., Pöschl, U., and Shiraiwa, M.: Molecular corridors and parameterizations of volatility in the chemical evolution of organic aerosols, *Atmos Chem Phys*, 16, 3327–3344, <https://doi.org/10.5194/acp-16-3327-2016>, 2016.
- 70 Lopez-Hilfiker, F. D., Mohr, C., Ehn, M., Rubach, F., Kleist, E., Wildt, J., Mentel, T. F., Lutz, A., Hallquist, M., Worsnop, D., and Thornton, J. A.: A novel method for online analysis of gas and particle composition: description and evaluation of a Filter Inlet for Gases and AEROsols (FIGAERO), *Atmos Meas Tech*, 7, 983–1001, <https://doi.org/10.5194/amt-7-983-2014>, 2014.